International Journal of Nanomedicine

Dovepress
open access to scientific and medical research

Open Access Full Text Article

ORIGINAL RESEARCH

Development of anisamide-targeted PEGylated gold nanorods to deliver epirubicin for chemo-photothermal therapy in tumor-bearing mice

This article was published in the following Dove Medical Press journal:
International Journal of Nanomedicine

Limei Wang,[1,2] Jin Pei,[1] Zhongcheng Cong,[1] Yifang Zou,[1] Tianmeng Sun,[3] Fionán Davitt,[4,5] Adrià Garcia-Gil,[4,5] Justin D Holmes,[4,5] Caitriona M O'Driscoll,[6] Kamil Rahme,[4,7] Jianfeng Guo[1]

[1]School of Pharmaceutical Sciences, Jilin University, Changchun 130021, China; [2]Department of Pharmacy, The General Hospital of FAW, Changchun 130011, China; [3]The First Hospital of Jilin University, Changchun 130021, China; [4]School of Chemistry and the Tyndall National Institute, University College Cork, Cork, Ireland; [5]CRANN, Trinity College Dublin, Dublin, Ireland; [6]Pharmacodelivery Group, School of Pharmacy, University College Cork, Cork, Ireland; [7]Department of Sciences, Faculty of Natural and Applied Science, Notre Dame University (Louaize), Zouk Mosbeh 1200, Lebanon

Correspondence: Jin Pei; Jianfeng Guo
School of Pharmaceutical Sciences, Jilin University, 1266 Fujin Road, Changchun 130021, China
Tel +86 431 8561 9725
Fax +86 431 8561 9252
Email peijin@jlu.edu.cn; jguo@jlu.edu.cn

Background: Gold nanorods (AuNRs), due to the optical and electronic properties namely the surface plasma resonance, have been developed to achieve the light-mediated photothermal therapy (PTT) for cancer. However, PTT alone may suffer from inefficient tumor killing. Recently, the combination of PTT and chemotherapy has been utilized to achieve synergistic anticancer effects.
Methods: In this study, AuNRs capped with hexadecyltrimethylammonium bromide (CTAB), poly(acrylic acid) (PAA), and PEGylated anisamide (a ligand known to target the sigma receptor) have been developed to produce a range of negatively charged anisamide-targeted PEGylated AuNRs (namely Au-CTAB-PAA-PEG-AA) for the combination of PTT and chemotherapy (termed as chemo-photothermal therapy [CPTT]). Epirubicin (EPI, an anthracycline drug) was efficiently loaded onto the surface of Au_{800}-CTAB-PAA-PEG-AA via the electrostatic interaction forming Au_{800}-CTAB-PAA-PEG-AA.EPI complex.
Results: The resultant complex demonstrated pH-dependent drug release, facilitated nucleus trafficking of EPI, and induced antiproliferative effects in human prostate cancer PC-3 cells. When Au_{800}-CTAB-PAA-PEG-AA.EPI complex was further stimulated with desired laser irradiation, the synergistic outcome was evident in PC-3 xenograft mice.
Conclusion: These results demonstrate a promising strategy for clinical application of CPTT in cancer.

Keywords: gold nanoparticles, non-viral drug delivery, chemotherapy, photothermal therapy, synergistic effect

Introduction

Nanomaterial-assisted photothermal therapy (PTT) has recently emerged as a potential therapeutic strategy for solid tumors. Due to the optical and electronic properties namely the surface plasma resonance (SPR), gold nanoparticles (AuNPs) with specific structures, including gold nanorods (AuNRs),[1] gold nanoshells,[2] and gold nanocages,[3] have been developed to absorb light strongly in certain wavelengths and convert the light energy into heat, resulting in cancer cell death by apoptosis and/or necrosis.[4] Among these nanostructures, AuNRs demonstrate unique physicochemical properties, in that they may strongly absorb light in wavelengths between 650 and 900 nm within the near-infrared (NIR) region.[5] It is known that for the light wavelengths between 650 and 2,000 nm, the tissue absorption is weak, and therefore tumors deeply seated within the body may be destroyed by PTT induced by AuNRs.[6] However, the heterogeneous heat distribution inside the tumors caused by the uneven distribution of AuNRs has curtailed the PTT efficacy. Therefore, novel therapeutic strategies are required to facilitate synergistic effects when combined with PTT.

submit your manuscript | www.dovepress.com
Dovepress
http://dx.doi.org/10.2147/IJN.S192520

Recently, the combination of PTT and other treatment modalities has presented great therapeutic potential for cancer. For instance, a variety of organic photosensitizers[7,8] can be loaded onto AuNRs; when photosensitizers are stimulated by the light of specific wavelengths, they convert the surrounding oxygen into toxic reactive oxygen species that may destroy cancer cells in surrounding proximity (known as photodynamic therapy [PDT]). The combination of AuNR-mediated PTT and photosensitizer-mediated PDT has demonstrated a significantly improved therapeutic efficacy.[7] In addition, the combination of chemotherapy with AuNR-mediated PTT (chemo-photothermal therapy [CPTT]) has also been confirmed to be more effective than either of the individual monotherapies.[9–16] However, the clinical application of CPTT is still retarded by significant delivery barriers, such as low drug loading efficiency, physiological instability, and lack of controlled drug release.[6] Therefore, the development of AuNRs with great potential both in drug delivery and PTT is highly needed.

In this study, AuNRs with tunable longitudinal SPR (λ_{max} =700, 725, 765, and 800 nm) were initially synthesized in the presence of hexadecyltrimethylammonium bromide (CTAB), which promotes the growth of gold seeds in one direction, to produce positively charged gold nanorods (Au-CTAB) (Figure 1). The Au-CTAB was subsequently coated by poly(acrylic acid) (PAA) to generate negatively charged Au-CTAB-PAA. To improve physiological stability and target cancer cells, Au-CTAB-PAA was further modified with PEGylated anisamide (AA, a ligand known to target the sigma receptor overexpressed on a variety of human cancers, such as breast cancer, melanoma, non-small-cell lung carcinoma, and prostate cancer)[17–19] to achieve Au-CTAB-PAA-PEG-AA (Figure 1). The Au-CTAB-PAA-PEG-AA was able to complex epirubicin (EPI, which is positively charged at physiological pH) via the electrostatic interaction forming Au-CTAB-PAA-PEG-AA.EPI complex. When stimulated with desired laser irradiation, the resultant complex of Au-CTAB-PAA-PEG-AA with EPI demonstrated significantly greater antitumor effects in a prostate tumor xenograft mouse model when compared to either of the individual monotherapies, providing a promising CPTT strategy for cancer therapy.

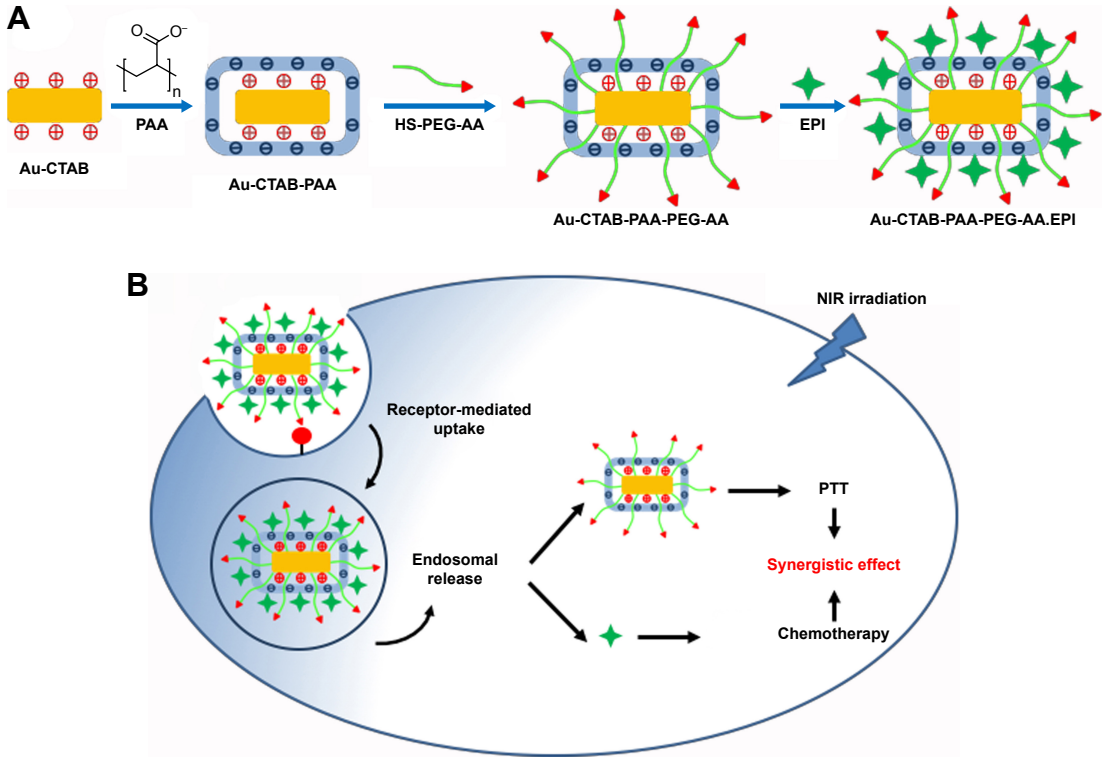

Figure 1 A schematic representation of anisamide-targeted PEGylated AuNRs for delivery of EPI to achieve photothermal therapy and chemotherapy in cancer.
Notes: (**A**) The scheme of anisamide-targeted AuNR.EPI formulation. (**B**) Targeted formulation will specifically bind sigma receptor, a well-known molecule overexpressing on the cell membrane of prostate cancer cells, achieving cellular uptake via receptor-mediated endocytosis. EPI will be released from targeted formulation in acidic environments (ie, endosomes). Following endosomal escape with the assistance of NIR irradiation, AuNRs may generate PTT, and EPI may enter the nucleus to induce chemotherapy. Consequently, the synergistic anticancer effect will be achieved using anisamide-targeted AuNR.EPI formulation.
Abbreviations: AuNRs, gold nanorods; EPI, epirubicin; NIR, near-infrared; CTAB, hexadecyltrimethylammonium bromide; PAA, poly(acrylic acid); AA, anisamide; PTT, photothermal therapy.

Materials and methods

Materials

PC-3 (human prostate cancer cell line) was purchased from the American Type Culture Collection (ATCC, Rockville, MD, USA). Epirubicin was purchased from Dalian Meilun Biotechnology (Dalian, China). Tetrachloroauric acid trihydrate ($HAuCl_4 \cdot 3H_2O$), L-ascorbic acid ($C_6H_8O_6$), sodium borohydride 99% ($NaBH_4$), silver nitrate ($AgNO_3$) >99%, CTAB ≥98%, sodium salt of PAA with average Mw ~2,100 Da, *O*-[2-(3-mercaptopropionylamino) ethyl]-*O′*-methylpolyethylene glycol 5000 ($SH\text{-}PEG_{5000}\text{-}OCH_3$), *N*-(3-dimethylaminopropyl)-*N′*-ethylcarbodiimide hydrochloride (EDC·HCl), N-hydroxysuccinimide (NHS), *N*,*N*-diisopropylethylamine (DIPEA) purified by redistillation, dry dichloromethane (DCM), dry pentane, and magnesium sulfate ($MgSO_4$) were purchased from Sigma-Aldrich Co. All chemicals were used as received without any further purification.

Synthesis of AuNRs

Purified H_2O (resistivity =18.2 MΩ cm) was used as a solvent for AuNR synthesis. Glassware was cleaned with aqua regia (3 parts of concentrated HCl and 1 part of concentrated HNO_3), rinsed with distilled water, ethanol, and acetone, and dried overnight before use.

Optical spectra

The optical absorption spectra were obtained using the Thermo Fisher™ Evolution™ 60S (Thermo Fisher Scientific, Waltham, MA, USA) UV-visible spectrophotometer with a xenon flash lamp (300–1,100 nm range, 0.5 nm resolution).

Scanning electron microscopy (SEM)

AuNRs were deposited onto a silicon wafer and air-dried prior to analysis using a FEI Quanta™ 650 equipped with an Oxford INCA energy-dispersive X-ray (EDX) detector operated at 5–20 kV and a high-resolution Helios DualBeam™ FIB Nanolab™ 600i equipped with an Oxford Aztec EDX detector operated at 5–30 kV.

Transmission electron microscopy (TEM)

AuNRs were deposited on carbon-coated copper grids (Ted Pella) and air-dried prior to TEM (JEOL JEM-2100 TEM operated at 200 kV). Images were recorded on a Gatan 1.35 K × 1.04 K ×12 bit ES500W CCD camera.

Dynamic light scattering

Particle size and zeta potential were measured in deionized water (0.2 μm membrane filter) using the Malvern Nano-ZS (Malvern Instruments, Malvern, UK) at 25°C with the default non-invasive back scattering technique at a detection angle of 173°.

Synthesis of AuNR-CTAB

Synthesis of AuNR-CTAB seeds: AuNRs capped with CTAB were synthesized by seed-mediated growth method.[20] Briefly, 5 mL of 0.5 mM $HAuCl_4$ solution was mixed with 5 mL of 0.2 M CTAB solution. About 0.6 mL of 0.01 M $NaBH_4$ freshly prepared in ice-cold water was added to the Au(III)-CTAB solution under vigorous stirring. The solution color changed to brownish yellow after the addition of $NaBH_4$ and the reaction was stopped after 2 minutes. The seed solution was aged at room temperature (RT) for 30 minutes before use.

Synthesis of AuNRs with longitudinal wavelength of ~800 nm: About 75 mL of 0.2 M CTAB solution was added to 3.75 mL of 4 mM $AgNO_3$ solution at 25°C, which was followed by the addition of 75 mL of 0.001 M $HAuCl_4$. Afterwards, 1.05 mL of 0.0788 M $C_6H_8O_6$ was added, and the solution color changed from dark yellow to colorless. Subsequently, 0.108 mL of the seed solution was added to the growth solution at 27°C–30°C. The solution color changed to reddish brown within 20–45 minutes. The growth medium was kept undisturbed at 27°C–30°C for 22 hours. The obtained AuNR-CTAB (hereafter referred to as Au_{800}-CTAB) was washed three times with deionized water by centrifugation (12,500 rpm, 5 minutes) prior to the following experiments.

The synthesis procedure of Au_{700}-CTAB, Au_{725}-CTAB, and Au_{765}-CTAB is described in the Supplementary materials.

Synthesis of NHS-activated anisic acid

NHS-activated anisic acid was produced as previously described.[21] Briefly, EDC·HCl (1.5 eq, 1.9 g, 9.9 mmol) was added to the *p*-anisic acid solution (6.572 mmol) in dry DCM (250 mL) under argon, followed by the addition of NHS (1.45 eq, 1.1 g, 9.56 mmol). The reaction mixture was stirred for ~42 hours under Argon at RT. The organic phase was washed twice with water followed by a wash with brine, dried over $MgSO_4$, filtered on Whatman filter paper, and evaporated. The activated ester thus obtained was left to stir in 30 mL of dry pentane for ~48 hours, filtered, dried under vacuum, and used without further purification. The yield of the anisic-NHS ester (AA-NHS) was ~90%. The product was analyzed using nuclear magnetic resonance (NMR) spectroscopy ([400 MHz, $CDCl_3$]: δ ppm 8.08–8.11

[d, 2H, ArH-CO–], 6.97–6.99 [d, 2H, ArH-OCH_3], 3.89 [s, 3H, OCH_3], 2.91 [s, 4H CH_2–CH_2 in NHS ring]).[21]

Synthesis of PEGylated anisamide (SH-PEG_{5000}-AA)

Hundred milligrams of SH-PEG_{5000}-NH_2 (0.02 mmol) was dried under the vacuum for 10 minutes at RT, followed by the application of a flow of nitrogen (N_2), and further dried under the vacuum for 5 minutes at RT. The SH-PEG_{5000}-NH_2 powder was then dissolved in 4 mL of DCM under N_2 and 2 mL of AA-NHS (0.034 mmol) in dry DCM was added and stirred at 0°C. Subsequently, 50 µL of DIPEA (0.688 mmol) in dry DCM was added and stirred under N_2 at RT for 48 hours. The resultant SH-PEG_{5000}-AA was precipitated at 0°C using 100 mL of cold diethyl ether/ethanol solution (v/v =99/1). The SH-PEG_{5000}-AA was collected at 0°C by centrifugation at 11,000 rpm and dried overnight under the vacuum. The SH-PEG_{5000}-AA (~90% yield) was characterized by NMR in $CDCl_3$: δ ppm 7.79–7.81 (d, 2H, ArH-CO–), 6.90–6.92 (d, 2H, ArH-OMethyl), 3.85 (s, Ar-OCH_3), 3.65 (O–CH_2–CH_2 of PEG), 2.9 (CH_2–C=O). The degree of anisamide attachment was ~100% as calculated from the peak integration ratio of phenyl proton at δ 7.78 to methylene protons at δ 3.65.

Synthesis of AuNR-CTAB-PAA, AuNR-CTAB-PAA-PEG, and AuNR-CTAB-PAA-PEG-AA

The resultant AuNR-CTAB was added into PAA solution (0.1–0.15 mM) at concentrations of 100–190 µg/mL to produce AuNR-CTAB-PAA. In addition, SH-PEG_{5000}-OCH_3 or SH-PEG_{5000}-AA (4 µM) was added into AuNR-CTAB-PAA to produce the final formulation Au-CTAB-PAA-PEG or Au-CTAB-PAA-PEG-AA at a molar ratio of 1:250 for SH-PEG_{5000}-OCH_3 or SH-PEG_{5000}-AA and $HAuCl_4$.

Preparation and physicochemical characterization of AuNR.EPI complex

In order to form AuNR.EPI complex, AuNRs (100 µg) were added to EPI solutions (0.5 µg/µL in 0.01 M PBS at pH =7.4) at different mass ratios (MRs), followed by 12-hour incubation with 400 rpm shaking at 45°C. Following incubation, the uncomplexed EPI was removed by centrifugation at 6,000 rpm for 20 minutes and measured using UV-visible spectrophotometer at 480 nm, in order to determine the efficiency of AuNRs to form complex with EPI. Particle size and zeta potential of AuNR.EPI complex were assessed using the Malvern Nano-ZS as described in the section "Dynamic light scattering".

In addition, the AuNR.EPI complex (MR =5) was incubated within the saline at 4°C and 37°C for 6, 24, and 48 hours. The particle size and zeta potential of AuNR.EPI complex were assessed using the Malvern Nano-ZS as described in the section "Dynamic light scattering".

To evaluate the photothermal conversion efficiency, 200 µL of PBS, EPI (0.2 µg/µL), blank AuNRs (1 µg/µL), and AuNR.EPI formulation (AuNR =1 µg/µL; MR =5) were irradiated by 808 nm NIR laser with an intensity of 2.5 W/cm^{-2} (BWT; Diode Laser System, Beijing, China). The temperature change was monitored by the infrared thermal analysis system (BM_IR; Beetech, Beijing, China) for 4.5 minutes at an interval of 0.5 min per reading.

In vitro release of EPI from AuNR.EPI complex

The Au_{800}-CTAB-PAA-PEG-AA.EPI complex (MR =5) was incubated in 0.01 M PBS (pH =5.5 and 7.4) at 37°C with 400 rpm shaking for 0.5, 1, 2, 4, 6, 12, 24, and 48 hours. At predetermined time intervals, the solution was centrifuged at 6,000 rpm for 20 minutes. About 200 µL of the supernatant was collected and replaced with the same volume of fresh release medium. The cumulative release rate of EPI was evaluated using high-performance liquid chromatography (SPD-20A; Shimadzu) at 480 nm.

Cellular uptake

PC-3 cells were maintained in RPMI-1640 medium (Corning Incorporated) supplemented with 10% FBS (heat inactivated; Thermo Fisher Scientific, Waltham, MA, USA) and 1% penicillin-streptomycin nystatin solution (Biological Industries). Cells (5×10^4 per well) were seeded in 24-well culture plates for 24 hours. Cells were then treated with Au_{800}-CTAB-PAA-PEG or Au_{800}-CTAB-PAA-PEG-AA (5 µg/mL) and incubated for 8 hours under normal growth conditions. Following incubation, cells were washed twice with PBS. Fresh growth medium was added to the cells prior to confocal microscopic analysis using an LSM 800 Zeiss confocal microscope (40×).

In addition, cells were also treated with Au_{800}-CTAB-PAA-PEG or Au_{800}-CTAB-PAA-PEG-AA (5 µg/mL) containing EPI (MR =5) and incubated for 4 hours under normal growth conditions. After this, cells were washed twice with PBS and trypsinized. After 1,000 rpm centrifugation for 5 minutes, the supernatant was discarded and cells were resuspended in 1,000 µL of ice-cold PBS. About 10,000 cells were measured to determine EPI-positive cells (%)

for each sample using flow cytometry (Becton Dickinson FACS-Canto II).

Intracellular trafficking

PC-3 cells were seeded in six-well culture plates with cover slip (CITOGLAS®, China) (2×10^5 cells per well) for 24 hours. Cells were then treated with EPI (1 μM) complexed with Au_{800}-CTAB-PAA-PEG-AA (MR =5) with/without laser irradiation (808 nm at 2.5 W/cm^2 for 0.5 minutes). Following 4 hours of incubation, cells were incubated in LysoTracker™ Green DND-26 (75 nM; Thermo Fisher Scientific) at 37°C for 30 minutes. Cells were washed twice with PBS and fixated with 350 μL paraformaldehyde (4%) in PBS for 20 minutes. Cells were then washed three times with PBS and treated with the mounting agent (SouthernBiotech). The confocal microscopic analysis was carried out using an LSM 800 Zeiss confocal microscope.

In vitro anticancer effects of AuNR.EPI complex

PC-3 cells (1×10^5 cells per well) were seeded in 24-well culture plates. Following 24 hours of incubation, cells were added by anisamide-targeted AuNRs (MR =5) complexed with or without 1 μM EPI for 12 hours. After this, cells were replaced with fresh growth medium and stimulated with 808 nm laser at 2.5 W/cm^2 for 0.5 minutes. Cells were further incubated for 12 hours under normal growth conditions. Subsequently, cells were lysed using RIPA buffer (50 mM Tris [pH 7.4], 150 mM NaCl, 1% NP-40, 0.5% sodium deoxycholate, 1% SDS, sodium orthovanadate, sodium fluoride, EDTA, and leupeptin), and protein concentrations were quantified using the Easy II BCA Protein Quantitative Kit (GenStar). Approximately 30–50 μg of proteins per sample was loaded onto an SDS-PAGE and electrophoresed at 80 V for 0.5 hours and subsequently at 120 V for 1.5 hours. Proteins were then transferred to a PVDF membrane (Immobilon®-P Transfer Membrane; EMD Millipore, Billerica, MA, USA) at 200 mA for 1.5 hours. Membranes were incubated with appropriate antibodies (caspase 3 [AF6311], cleaved caspase 3 [AF7022], caspase 9 [AF6348], cleaved caspase 9 [AF5240], Bax [AF0120], Bcl-2 [AF6139], and β-actin [AF7018], purchased from Affinity Biosciences, Cincinnati, OH, USA) at RT for 12 hours. Antibody reactive bands were detected using MicroChemi (DNR Bio-Imaging Systems Ltd., Jerusalem, Israel). Densitometry analysis of bands was performed using ImageJ, and all results were normalized to the β-actin control.

In addition, PC-3 cells (5×10^3 per well) were seeded in 96-well plates for 1 day. After this, cells were treated with EPI (1 μM), Au-CTAB-PAA-PEG (MR =5) complexed with or without EPI, and Au-CTAB-PAA-PEG-AA (MR =5) complexed with or without EPI. After 8 hours of incubation, cells were replaced with fresh growth medium and stimulated with 808 nm laser at 2.5 W/cm^2 for 0.5 minutes. Cells were further incubated for 24 and 48 hours under normal growth conditions. Cells were then added with 20 μL MTT stock (5 mg/mL in PBS) in 200 μL of fresh growth medium and incubated for 3–4 hours at 37°C. About 150 μL of DMSO was added to dissolve the purple formazan products. The results were read at 570 nm using microplate reader.

In vivo antitumor efficacy of AuNR.EPI complex

All animals received care in compliance with the guidelines outlined in the Guide for the Care and Use of Laboratory Animals. The animal ethics committee of Jilin University approved all experiments. All mice were maintained in a pathogen-free animal facility for at least 2 weeks before the experiments.

Male BALB/c nude mice (5–6 weeks) were purchased from Beijing Vital River Laboratory Animal Technology Co., Ltd. The xenograft mice were established by subcutaneous injection of 5×10^6 PC-3 cells into the flank of animals. The tumor volume was calculated using the formula $a^2b(\pi/6)$, where a is the minor diameter of the tumor and b is the major diameter perpendicular to diameter a. When the tumor reached a volume of ~200 mm^3 (day 0), mice (n=4 per group) were intratumorally injected at days 1, 3, 5, 7, and 9 with saline, Au_{800}-CTAB-PAA-PEG-AA (2.5 mg/kg) followed by 808 nm laser stimulation at 2.5 W/cm^2 for 2 minutes, and Au_{800}-CTAB-PAA-PEG-AA (MR =5) containing EPI (0.5 mg/kg) with or without the 808 nm laser stimulation at 2.5 W/cm^2 for 2 minutes. Tumor growth and body weight were recorded regularly, and the tumor volume was calculated as described earlier.

Statistical analyses

Data were calculated as the mean ± SD. An unpaired Student's *t*-test (two-tailed) was used to test the significance of differences between two mean values. A one-way ANOVA (Bonferroni's post hoc test) was used to test the significance of differences in three or more groups. In addition, a two-way ANOVA (Bonferroni's post hoc test) was used to test the significance of differences in measurements of body weight,

pharmacokinetics, and tumor growth. In all experiments, $P<0.05$ was considered statistically significant.

Results and discussion

Synthesis and physicochemical characterization of AuNRs

Recently, nanomaterial-based PTT has demonstrated great potential for cancer therapy.[22] AuNRs, due to the tunable and sensitive SPR, have been developed to absorb the NIR irradiation for light to heat conversion,[23] providing the thermal ablation of malignant cells (more thermosensitive cells),[24] while causing less subversion to the surrounding healthy cells.

In this study, AuNRs with tunable longitudinal SPR (λ_{max} =700–800 nm) were initially synthesized via seeding growth method in the presence of CTAB as shape directing agent to produce positively charged Au-CTAB (Figures 2A, B and S1). The formation of Au-CTAB was confirmed by UV-vis spectroscopy indicating that AuNR-CTAB had different maximum of absorption at 700, 725, 765, and 800 nm, respectively, with different aspect ratios (Figure 2C). These Au-CTAB NPs were subsequently coated by a polyelectrolyte PAA to generate negatively charged Au-CTAB-PAA. As shown in Figure 2D, Au_{800}-CTAB-PAA demonstrated a negatively charged surface (–47 mV) compared to Au_{800}-CTAB (40 mV), indicating the successful deposition of anionic PAA onto the cationic surface of Au-CTAB.

Sigma receptors are well known to overexpress on the membrane of various human cancer cells (eg, breast cancer, melanoma, non-small-cell lung carcinoma, and prostate cancer).[25,26] Recently, NPs modified with anisamide or anisamide derivatives for targeting sigma receptors have shown promise for efficient drug delivery in the treatment of cancer.[27–33] As shown in Figure 2D, the zeta potentials of Au_{800}-CTAB-PAA-PEG and Au_{800}-CTAB-PAA-PEG-AA were –18 mV and –25 mV respectively, which were significantly higher than that of Au_{800}-CTAB-PAA (–47 mV), indicating that the surface of Au-CTAB-PAA has been further modified with SH-PEG_{5000}-OCH_3 and SH-PEG_{5000}-AA (Figures S2 and S3). In addition, a "halo-like" layer was clearly observed on the surface of Au-CTAB-PAA-PEG-AA (Figure 2E), most likely due to the attachment

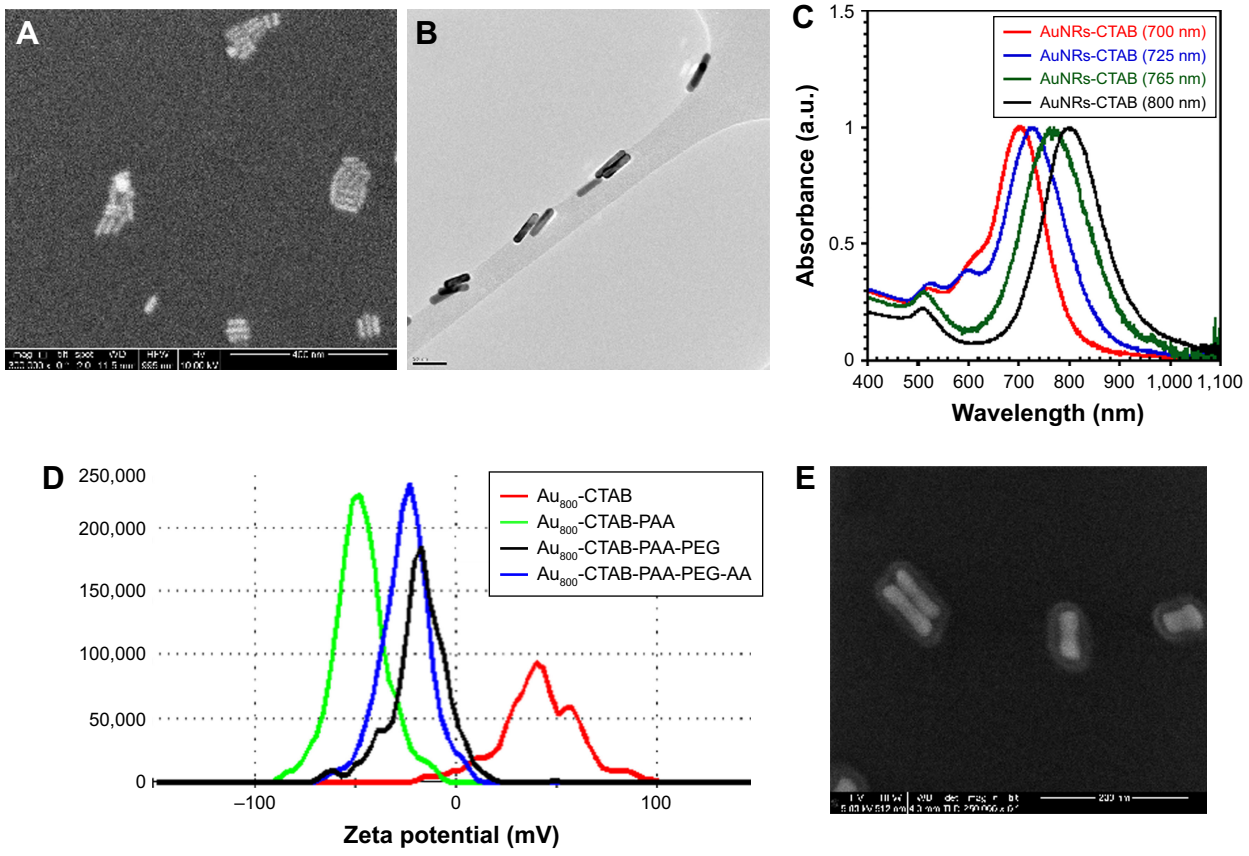

Figure 2 (**A**) SEM of Au_{800}-CTAB (scale bar =400 nm); (**B**) TEM of Au_{800}-CTAB (scale bar =50 nm); (**C**) UV-vis spectrum of Au_{700}-CTAB, Au_{725}-CTAB, Au_{765}-CTAB, and Au_{800}-CTAB; (**D**) zeta potential of Au_{800}-CTAB, Au_{800}-CTAB-PAA, Au_{800}-CTAB-PAA-PEG, and Au_{800}-CTAB-PAA-PEG-AA obtained using the Malvern Nano-ZS; (**E**) high-energy SEM of Au_{800}-CTAB-PAA-PEG-AA (scale bar =200 nm).

Abbreviations: AuNRs, gold nanorods; SEM, scanning electron microscopy; CTAB, hexadecyltrimethylammonium bromide; PAA, poly(acrylic acid); AA, anisamide; TEM, transmission electron microscopy; PEG, polyethylene glycol.

of SH-PEG$_{5000}$-AA. Therefore, these results show that the PEGylated anisamide was successfully conjugated onto the surface of Au-CTAB-PAA forming Au-CTAB-PAA-PEG-AA. In addition, the PEGylated AuNRs were stable for >1 year when stored in the dark at 4°C.

Formulation and physicochemical characterization of AuNR.EPI complex

Doxorubicin (DOX) is a commonly used chemotherapeutic for a diverse set of human cancers, and can result in antiproliferative actions by blocking the topoisomerase I/II activity and by intercalating into DNA. DOX, due to cationic property in physiological environments,[34] could be loaded onto the surface of negatively charged NPs. EPI (an epimer of DOX) has similar therapeutic efficacy with DOX, but causes less cardiotoxicity and myelosuppression compared to DOX.[35] Therefore, EPI was chosen to achieve the complexation with Au-CTAB-PAA-PEG-AA via the electrostatic interaction.

The complexation efficiency of EPI with PEGylated AuNRs was optimized at MR 5 of AuNRs and EPI. As shown in Table 1, Au$_{800}$-CTAB-PAA-PEG and Au$_{800}$-CTAB-PAA-PEG-AA demonstrated ~90% complexation efficiency of EPI at MR 5, which was significantly higher (~65%) than those of Au$_{700}$-CTAB-PAA-PEG and Au$_{700}$-CTAB-PAA-PEG-AA. It is interesting to note that aggregation occurred to PEGylated AuNRs with λ_{max} =725 and 765 nm (Table 1). In comparison to AuNRs, the net charges of AuNR.EPI complexes were significantly increased when complexed with EPI (~10 mV) (Table 1). These results indicate that cationic EPI was electrostatically complexed onto the anionic surface of PEGylated AuNRs. On the basis of the physicochemical results, the complexes of Au$_{800}$-CTAB-PAA-PEG-AA with EPI at MR 5 were used for the following in vitro and in vivo experiments.

The SPR is dependent on size and shape of AuNRs, and therefore the morphological stability of AuNRs is of importance for PTT application. The incorporation of PEG into NPs is known to enhance the stability in physiological environments.[36,37] In this study, when PEGylated AuNR.EPI complexes (MR =5) were incubated with saline at 4°C and 37°C, no significant NP aggregation was observed up to 48 hours (Figure S4), implying the ability of PEGylated AuNR.EPI complexes to stabilize nanostructures in vitro and in vivo.

A safe and efficient delivery system allows drug release inside cancer cells, but avoids burst release during blood circulation. In order to investigate the release profiles, EPI complexed with Au$_{800}$-CTAB-PAA-PEG-AA was incubated with 0.01 M PBS (pH =5.5 and 7.4) at 37°C with 400 rpm shaking. As shown in Figure 3, no burst release of EPI from anisamide-targeted AuNRs was observed at pH =7.4, and in contrast, a pH change from 7.4 to 5.5 significantly increased the release rate (by approximately fourfold). These results suggest that anisamide-targeted AuNRs may avoid the burst release of EPI in the physiological environments (pH =7.4) but facilitate the drug release inside endosomes (pH =5.5) of cancer cells.

Table 1 Physicochemical characterization of AuNRs and AuNR.EPI complexes (MR =5) (n=5)

AuNRs	Particle size (nm)	Zeta potential (mV)	Complexation efficiency (%)
Au$_{700}$-CTAB-PAA-PEG	25±1 (PDI =0.174)	−21±1	N/T
Au$_{700}$-CTAB-PAA-PEG.EPI	80±2 (PDI =0.235)	−6±2	68±5
Au$_{700}$-CTAB-PAA-PEG-AA	33±2 (PDI =0.152)	−20±1	N/T
Au$_{700}$-CTAB-PAA-PEG-AA.EPI	85±2 (PDI =0.260)	−5±2	65±3
Au$_{725}$-CTAB-PAA-PEG	22±1 (PDI =0.174)	−18±2	N/T
Au$_{725}$-CTAB-PAA-PEG.EPI	Aggregation	N/T	N/T
Au$_{725}$-CTAB-PAA-PEG-AA	31±1 (PDI =0.174)	−17±2	N/T
Au$_{725}$-CTAB-PAA-PEG-AA.EPI	Aggregation	N/T	N/T
Au$_{765}$-CTAB-PAA-PEG	24±3 (PDI =0.184)	−17±3	N/T
Au$_{765}$-CTAB-PAA-PEG.EPI	Aggregation	N/T	N/T
Au$_{765}$-CTAB-PAA-PEG-AA	35±3 (PDI =0.182)	−19±3	N/T
Au$_{765}$-CTAB-PAA-PEG-AA.EPI	Aggregation	N/T	N/T
Au$_{800}$-CTAB-PAA-PEG	24±3 (PDI =0.170)	−22±3	N/T
Au$_{800}$-CTAB-PAA-PEG.EPI	82±2 (PDI =0.235)	−5±1	91±2
Au$_{800}$-CTAB-PAA-PEG-AA	36±2 (PDI =0.160)	−19±2	N/T
Au$_{800}$-CTAB-PAA-PEG-AA.EPI	90±2 (PDI =0.229)	−5±1	90±3

Abbreviations: AuNRs, gold nanorods; EPI, epirubicin; MR, mass ratio; PDI, polydispersity index; N/T, not tested; CTAB, hexadecyltrimethylammonium bromide; PAA, poly(acrylic acid); AA, anisamide; PEG, polyethylene glycol.

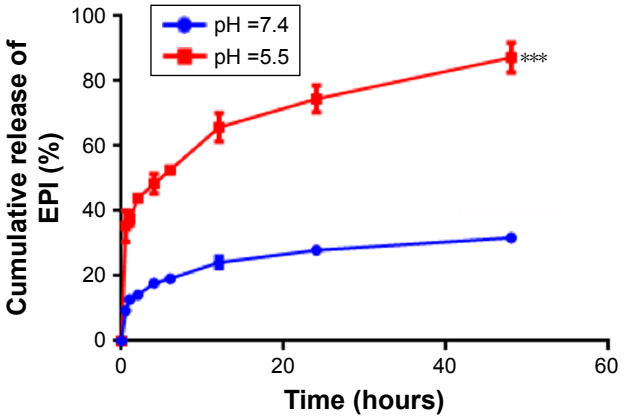

Figure 3 The in vitro release of EPI from Au_{800}-CTAB-PAA-PEG-AA (MR =5) in pH =5.5 and 7.4 at 37°C with 400 rpm shaking (n=5; ***$P<0.001$).
Abbreviations: Au, gold; EPI, epirubicin; MR, mass ratio; CTAB, hexadecyltrimethylammonium bromide; PAA, poly(acrylic acid); AA, anisamide; PEG, polyethylene glycol.

Cellular uptake and intracellular trafficking

PC-3, a sigma receptor overexpressing cell line,[19,21,38,39] was therefore chosen to investigate in vitro and in vivo potential of anisamide-targeted AuNRs. AuNPs are known as a very useful contrast agent and can be visualized using differential interference contrast (DIC) microscopy.[40] Indeed, DIC microscopy has been commonly used to investigate the cellular uptake of AuNPs.[41–43] As shown in Figure 4A, DIC images demonstrate that anisamide-targeted AuNRs (detected as dark dots)[41–43] significantly enhanced the uptake into PC-3 cells relative to untreated cells or cells treated with non-targeted counterparts in which minor AuNRs were observed (Figure 4A), suggesting a receptor-mediated cellular uptake due to the attachment of anisamide targeting ligand.

In addition, EPI was used to further investigate the cellular uptake of Au_{800}-CTAB-PAA-PEG-AA complex in PC-3 cells (Figure 4B).[44] The results of flow cytometry displayed a significantly higher cellular uptake of anisamide-targeted AuNR.EPI formulation when compared to untreated group and non-targeted AuNR.EPI formulation (Figure 4B). These results further confirm that grafting of anisamide may enhance targeting of AuNRs to PC-3 cells through the sigma receptor-associated pathway.

Following ligand–receptor mediated internalization, NPs are normally transported into endosomes in which the pH becomes ~5–6. It is known that DOX, as a basic chemotherapeutic, is membrane permeable in the neutral form

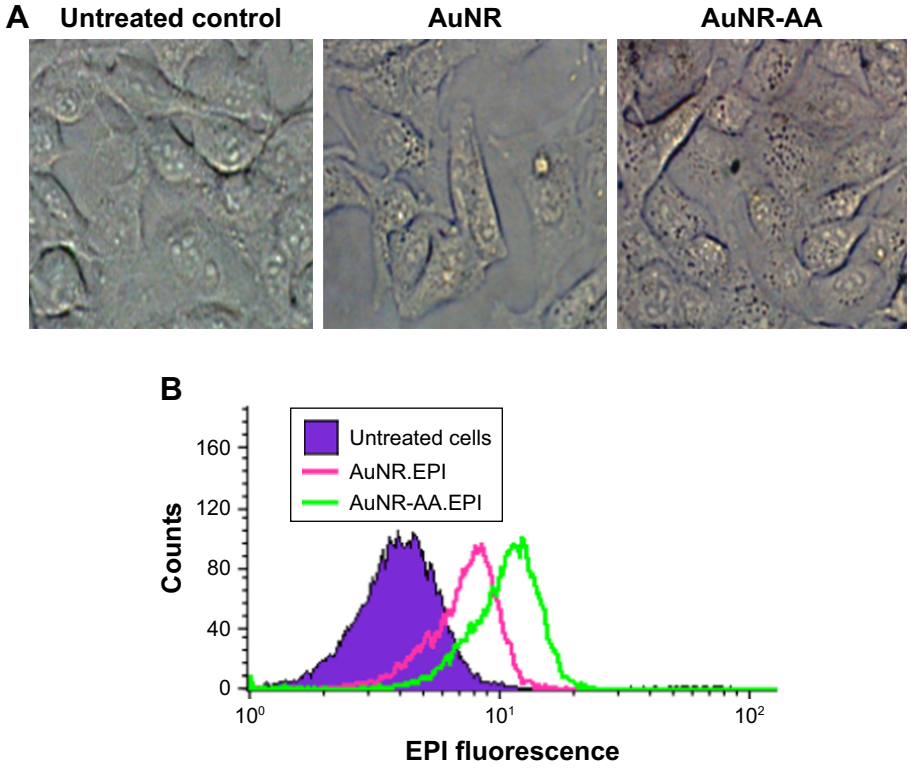

Figure 4 Cellular uptake of anisamide-targeted AuNRs in PC-3 cells was measured using (**A**) confocal microscopy and (**B**) flow cytometry.
Note: The images were acquired using an LSM 800 Zeiss confocal microscope (40×).
Abbreviations: AuNRs, gold nanorods; EPI, epirubicin; CTAB, hexadecyltrimethylammonium bromide; PAA, poly(acrylic acid); AA, anisamide; PEG, polyethylene glycol.

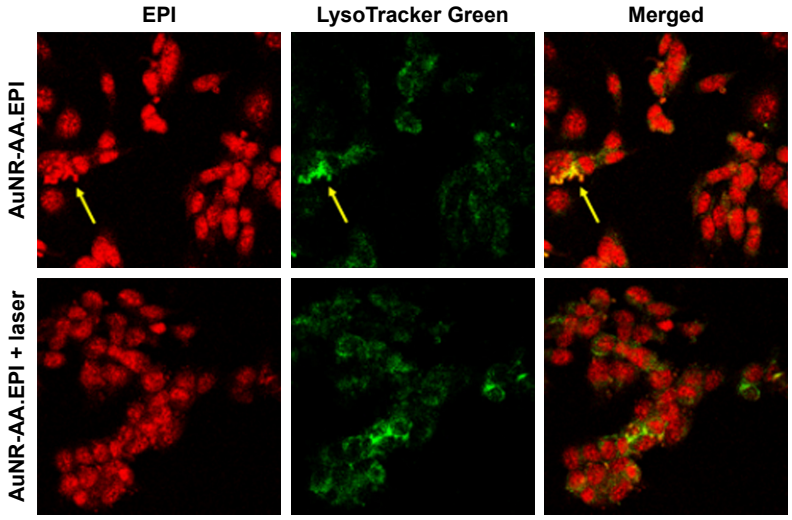

Figure 5 Intracellular distribution of anisamide-targeted AuNRs in PC-3 cells.
Notes: PC-3 cells were treated with 5 μg/mL of Au_{800}-CTAB-PAA-PEG or Au_{800}-CTAB-PAA-PEG-AA and incubated for 4 hours. A definite fraction of EPI (red) was detected inside endosomes/lysosomes (green) (as indicated by yellow arrows) for targeted AuNR.EPI complex (MR =5). Following the laser irradiation at 808 nm at 2.5 W/cm^2 for 0.5 minutes, no obvious co-localization of red and green fluorescence was evident in cells treated with targeted AuNR.EPI complex, and EPI was clearly found inside the nucleus. The images were acquired using an LSM 800 Zeiss confocal microscope (40×).
Abbreviations: AuNRs, gold nanorods; EPI, epirubicin; CTAB, hexadecyltrimethylammonium bromide; PAA, poly(acrylic acid); AA, anisamide; PEG, polyethylene glycol; MR, mass ratio.

but relatively impermeable when protonated.[45] Therefore, when DOX or EPI enter into acidic endosomes, they become protonated and are subsequently sequestered.[46] As shown in Figure 5, a definite fraction of EPI (red) was detected inside endosomes/lysosomes (green) (as indicated by yellow arrows) for targeted AuNR.EPI complex (MR =5). It has been reported that photothermal activation can be employed to enhance endosomal escape of therapeutic cargos.[47,48] As shown in Figure 2, Au_{800}-CTAB-PAA-PEG-AA exhibited a SPR in response to the wavelength of 800 nm. When stimulated with laser irradiation at 808 nm, 2.5 W/cm^2 for 0.5 minutes, the surface temperature of Au_{800}-CTAB-PAA-PEG-AA and Au_{800}-CTAB-PAA-PEG-AA.EPI was increased to ~55°C and ~65°C, respectively (Figure S5), and such temperature is sufficient for hyperthermal effect. Indeed, following the laser irradiation, no obvious co-localization of red and green fluorescence was evident in cells treated with targeted AuNR.EPI complex (Figure 5), indicating the potential of AuNR-based photothermally induced endosomal release of EPI.

In vitro anticancer efficacy

To investigate the capacity of anisamide-targeted AuNR.EPI formulation to induce apoptosis, the expression of Bcl-2 and Bax and the activity of caspases 9 and 3 were assessed using Western blotting of PC-3 cells (Figures 6 and S6). The expression of Bcl-2 (one anti-apoptotic mediator)[49] was significantly reduced by anisamide-targeted AuNR.EPI formulation (Figures 6 and S6). It has been reported that thermal therapy (also called hyperthermia) may increase the sensitivity of cancer cells to DOX and EPI,[50] as hyperthermia can retard the repair of DNA damage caused by anthracycline antibiotics.[51] Indeed, when stimulated with

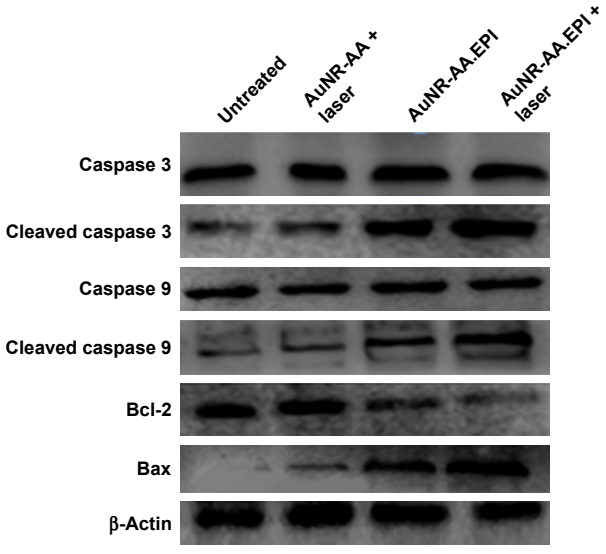

Figure 6 The expression of caspase 3, cleaved caspase 3 (phosphorylated form), caspase 9, cleaved caspase 9 (phosphorylated form), Bcl-2, Bax, and β-actin was determined using Western blotting.
Note: Untreated = untreated cells; AuNR-AA + laser = Au_{800}-CTAB-PAA-PEG-AA plus laser irradiation; AuNR-AA.EPI = Au_{800}-CTAB-PAA-PEG-AA.EPI; and AuNR-AA.EPI + laser = Au_{800}-CTAB-PAA-PEG-AA.EPI plus laser irradiation.
Abbreviations: AuNRs, gold nanorods; EPI, epirubicin; CTAB, hexadecyltrimethylammonium bromide; PAA, poly(acrylic acid); AA, anisamide; PEG, polyethylene glycol.

laser irradiation, EPI complexed with anisamide-targeted AuNRs further reduced the expression of Bcl-2 (Figures 6 and S6). It is known that Bcl-2 is functional to restrain pro-apoptotic Bax/Bak.[49] Following the downregulation of Bcl-2, the expression of Bax was significantly enhanced by anisamide-targeted AuNR.EPI complex plus laser irradiation (Figures 6 and S6). It is known that Bax can activate caspase 9, and once activated, caspase 9 induces the downstream "apoptosis-effector caspases" (ie, caspase 3). As shown in Figures 6 and S6, the anisamide-targeted AuNR.EPI complex plus laser irradiation significantly improved the activity of caspase 9/3 relative to either of monotherapies. This synergistic apoptotic effect confirmed the hypothesis that the laser-based thermal activation induced by anisamide-targeted AuNRs can enhance the sensitivity of tumor cells to EPI.

Due to the apoptotic effects, targeted AuNR.EPI complex (MR =5) with laser treatment significantly slowed down the proliferation of PC-3 cells ($P<0.01$; <50% and >70% reductions after 24 hours and 48 hours incubation, respectively) (Figure 7); in contrast, less cytotoxicity was observed with either of monotherapies. In addition, the targeted complex achieved significantly higher cell death relative to its non-targeted counterpart (Figure 7), further indicating the function of anisamide targeting ligand.

As AuNRs alone did not cause any cytotoxicity (Figure 7), the in vitro anticancer effect achieved with anisamide-targeted AuNR.EPI complex plus laser irradiation was most likely due to the synergistic apoptotic effects.

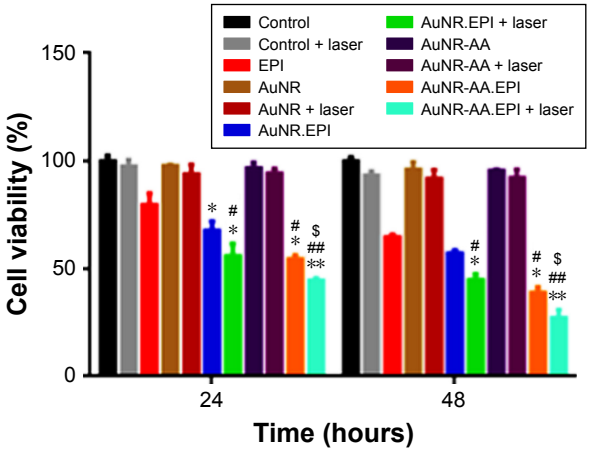

Figure 7 Cell viability measured in PC-3 cells after 24 hours and 48 hours of treatment with anisamide-targeted AuNR.EPI complex plus laser irradiation (808 nm at 2.5 W/cm^2 for 0.5 minutes) using MTT assay (n=3). EPI =1 μM; AuNR = Au_{800}-CTAB-PAA-PEG; AuNR.EPI = Au_{800}-CTAB-PAA-PEG.EPI (MR =5); AuNR-AA = Au_{800}-CTAB-PAA-PEG-AA; and AuNR-AA.EPI = Au_{800}-CTAB-PAA-PEG-AA.EPI (MR =5). *$P<0.05$ and **$P<0.01$ relative to EPI; #$P<0.05$ and ##$P<0.01$ relative to AuNR.EPI; $$P<0.0$ relative to AuNR-AA.EPI.

Abbreviations: AuNRs, gold nanorods; EPI, epirubicin; CTAB, hexadecyltrimethylammonium bromide; PAA, poly(acrylic acid); AA, anisamide; PEG, polyethylene glycol; MR, mass ratio.

In vivo antitumor efficacy

Recently, the combination of chemotherapy with AuNR-mediated PTT has been confirmed to be more effective than either of the individual therapies.[9–16] In this study, the anisamide-targeted AuNR-based CPTT efficacy was assessed in subcutaneous PC-3 xenograft mice following intratumoral injection (n=4) (Figure 8A and B). Results show that both Au_{800}-CTAB-PEG-AA complex containing EPI (MR =5) and Au_{800}-CTAB-PEG-AA with laser stimulation significantly ($P<0.05$) slowed down tumor growth relative to the saline control group. In addition, when stimulated with laser irradiation, the Au_{800}-CTAB-PEG-AA.EPI complex further ($P<0.05$) retarded tumor growth compared to either of monotherapies. Records of mouse body weight demonstrated no significant loss compared to the saline control group over the treatment period (Figure 8C), indicating the absence of AuNR-induced toxicity. These results indicate that the combination of anisamide-targeted AuNR-based PTT and simultaneous application of EPI may provide the synergistic therapeutic potential for the treatment of sigma receptor-positive prostate carcinoma.

Conclusion

A range of negatively charged anisamide-targeted PEGylated AuNRs (namely Au-CTAB-PAA-PEG-AA) were developed for PTT and simultaneous delivery of EPI in the treatment of cancer (Figure 1). One of the Au-CTAB-PAA-PEG-AA combinations, namely Au_{800}-CTAB-PAA-PEG-AA, could effectively complex EPI via the electrostatic interaction, and the resultant complexation (Au_{800}-CTAB-PAA-PEG-AA.EPI) demonstrated favorable particle size, surface charge, and stability. Au_{800}-CTAB-PAA-PEG-AA.EPI demonstrated efficient release of EPI in acidic buffer solution but avoided burst drug release in physiological buffer solution, demonstrating the role of anisamide-targeted AuNRs as the controlled drug delivery system. The in vitro studies showed cell-specific internalization indicating the function of the anisamide targeting ligand. When stimulated with desired laser irradiation, the anisamide-targeted AuNR.EPI complex demonstrated in vivo synergistic antitumor effects in PC-3 xenografted mice compared to either of individual monotherapies, without showing significant toxicity. These results imply that the anisamide-targeted AuNR vector provides a promising strategy for combination of chemotherapy and PTT in the treatment of sigma receptor-positive cancer.

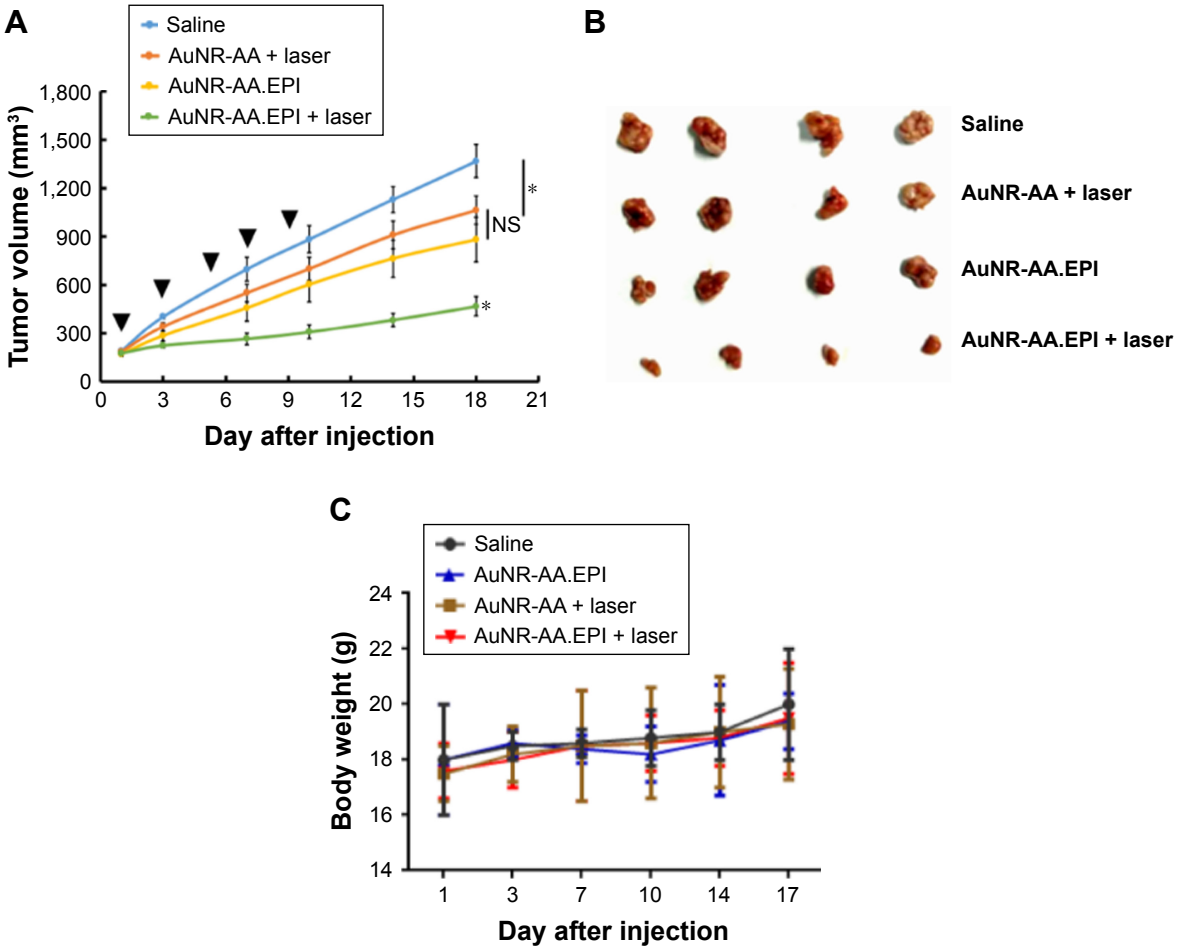

Figure 8 (**A**) PC-3 xenograft mice (n=4 per group) following intratumoral injections of Au_{800}-CTAB-PAA-PEG-AA.EPI (MR 5; ~0.5 mg/kg EPI) followed by 808 nm laser stimulation at 2.5 W/cm² for 2 minutes on days 1, 3, 5, 7, and 9. (**B**) The image of tumors was obtained at day 17. (**C**) At predetermined days, body weight (mean ± SD, n=4) was recorded to determine in vivo toxicity (*$P<0.05$).

Abbreviations: AuNRs, gold nanorods; EPI, epirubicin; CTAB, hexadecyltrimethylammonium bromide; PAA, poly(acrylic acid); AA, anisamide; PEG, polyethylene glycol; MR, mass ratio; NS, not significant.

Acknowledgments

This work was supported by the Outstanding Youth Foundation from the Department of Science and Technology, Jilin Province, China (20170520046JH), the Start-Up Research Grant Program from Jilin University (451170301168, 451160102052, 419080500667), and the Fundamental Research Funds for the Central Universities, China. Jin Pei, Kamil Rahme and Jianfeng Guo are co-corresponding authors.

Disclosure

The authors report no conflicts of interest in this work.

References

1. Huang X, Neretina S, El-Sayed MA. Gold nanorods: from synthesis and properties to biological and biomedical applications. *Adv Mater*. 2009;21(48):4880–4910.
2. Lal S, Clare SE, Halas NJ. Nanoshell-enabled photothermal cancer therapy: impending clinical impact. *Acc Chem Res*. 2008;41(12):1842–1851.
3. Chen J, Glaus C, Laforest R, et al. Gold nanocages as photothermal transducers for cancer treatment. *Small*. 2010;6(7):811–817.
4. Ali MR, Rahman MA, Wu Y, et al. Efficacy, long-term toxicity, and mechanistic studies of gold nanorods photothermal therapy of cancer in xenograft mice. *Proc Natl Acad Sci U S A*. 2017;114(15):E3110–E3118.
5. Alkilany AM, Thompson LB, Boulos SP, Sisco PN, Murphy CJ. Gold nanorods: their potential for photothermal therapeutics and drug delivery, tempered by the complexity of their biological interactions. *Adv Drug Deliv Rev*. 2012;64(2):190–199.
6. Guo J, Rahme K, He Y, Li LL, Holmes JD, O'Driscoll CM. Gold nanoparticles enlighten the future of cancer theranostics. *Int J Nanomedicine*. 2017;12:6131–6152.
7. Chen R, Wang X, Yao X, Zheng X, Wang J, Jiang X. Near-IR-triggered photothermal/photodynamic dual-modality therapy system via chitosan hybrid nanospheres. *Biomaterials*. 2013;34(33):8314–8322.
8. Jayaram DT, Ramos-Romero S, Shankar BH, et al. In vitro and in vivo demonstration of photodynamic activity and cytoplasm imaging through tpe nanoparticles. *ACS Chem Biol*. 2016;11(1):104–112.
9. Cheng FY, Su CH, Wu PC, Yeh CS. Multifunctional polymeric nanoparticles for combined chemotherapeutic and near-infrared photothermal cancer therapy in vitro and in vivo. *Chem Commun*. 2010;46(18):3167–3169.
10. Kuo TR, Hovhannisyan VA, Chao YC, et al. Multiple release kinetics of targeted drug from gold nanorod embedded polyelectrolyte conjugates induced by near-infrared laser irradiation. *J Am Chem Soc*. 2010;132(40):14163–14171.

11. Hribar KC, Lee MH, Lee D, Burdick JA. Enhanced release of small molecules from near-infrared light responsive polymer-nanorod composites. *ACS Nano*. 2011;5(4):2948–2956.
12. Ren F, Bhana S, Norman DD, et al. Gold nanorods carrying paclitaxel for photothermal-chemotherapy of cancer. *Bioconjug Chem*. 2013;24(3):376–386.
13. Monem AS, Elbialy N, Mohamed N. Mesoporous silica coated gold nanorods loaded doxorubicin for combined chemo-photothermal therapy. *Int J Pharm*. 2014;470(1–2):1–7.
14. Hua H, Zhang N, Liu D, et al. Multifunctional gold nanorods and docetaxel-encapsulated liposomes for combined thermo- and chemotherapy. *Int J Nanomedicine*. 2017;12:7869–7884.
15. Chen J, Li X, Zhao X, et al. Doxorubicin-conjugated pH-responsive gold nanorods for combined photothermal therapy and chemotherapy of cancer. *Bioact Mater*. 2018;3(3):347–354.
16. Wang X, Gao S, Qin Z, et al. Evans blue derivative-functionalized gold nanorods for photothermal Therapy-Enhanced tumor chemotherapy. *ACS Appl Mater Interfaces*. 2018;10(17):15140–15149.
17. Vilner BJ, John CS, Bowen WD. Sigma-1 and sigma-2 receptors are expressed in a wide variety of human and rodent tumor cell lines. *Cancer Res*. 1995;55(2):408–413.
18. Banerjee R, Tyagi P, Li S, Huang L. Anisamide-targeted stealth liposomes: a potent carrier for targeting doxorubicin to human prostate cancer cells. *Int J Cancer*. 2004;112(4):693–700.
19. Guo J, Ogier JR, Desgranges S, Darcy R, O'Driscoll C. Anisamide-targeted cyclodextrin nanoparticles for siRNA delivery to prostate tumours in mice. *Biomaterials*. 2012;33(31):7775–7784.
20. Nikoobakht B, El-Sayed MA. Preparation and growth mechanism of gold nanorods (NRS) using seed-mediated growth method. *Chem Mater*. 2003;15(10):1957–1962.
21. Fitzgerald KA, Rahme K, Guo J, Holmes JD, O'Driscoll CM. Anisamide-targeted gold nanoparticles for siRNA delivery in prostate cancer – synthesis, physicochemical characterisation and in vitro evaluation. *J Mater Chem*. 2016;4(13):2242–2252.
22. Hussein E, Zagho M, Nasrallah G, Elzatahry A. Recent advances in functional nanostructures as cancer photothermal therapy. *Int J Nanomed*. 2018;13:2897–2906.
23. Riley RS, Day ES. Gold nanoparticle-mediated photothermal therapy: applications and opportunities for multimodal cancer treatment. *WIREs Nanomed Nanobiotechnol*. 2017;9(4):e1449.
24. Cabral RM, Baptista PV. Anti-cancer precision theranostics: a focus on multifunctional gold nanoparticles. *Expert Rev Mol Diagn*. 2014;14(8):1041–1052.
25. Kim FJ, Maher CM. Sigma1 pharmacology in the context of cancer. *Handb Exp Pharmacol*. 2017;244:237–308.
26. Rousseaux CG, Greene SF. Sigma receptors [σRs]: biology in normal and diseased states. *J Recept Signal Transduct Res*. 2016;36(4):327–388.
27. Chen Y, Bathula SR, Yang Q, Huang L. Targeted nanoparticles deliver siRNA to melanoma. *J Invest Dermatol*. 2010;130(12):2790–2798.
28. Wang Y, Su HH, Yang Y, et al. Systemic delivery of modified mRNA encoding herpes simplex virus 1 thymidine kinase for targeted cancer gene therapy. *Mol Ther*. 2013;21(2):358–367.
29. Rodriguez BL, Blando JM, Lansakara-P DSP, Kiguchi Y, Digiovanni J, Cui Z. Antitumor activity of tumor-targeted RNA replicase-based plasmid that expresses interleukin-2 in a murine melanoma model. *Mol Pharm*. 2013;10(6):2404–2415.
30. Fitzgerald KA, Malhotra M, Gooding M, et al. A novel, anisamide-targeted cyclodextrin nanoformulation for siRNA delivery to prostate cancer cells expressing the sigma-1 receptor. *Int J Pharm*. 2016;499(1–2):131–145.
31. Evans JC, Malhotra M, Fitzgerald KA, et al. Formulation and evaluation of Anisamide-Targeted amphiphilic cyclodextrin nanoparticles to promote therapeutic gene silencing in a 3D prostate cancer bone metastases model. *Mol Pharm*. 2017;14(1):42–52.
32. Liu Q, Zhu H, Tiruthani K, et al. Nanoparticle-Mediated trapping of Wnt family member 5A in tumor microenvironments enhances immunotherapy for B-Raf proto-oncogene mutant melanoma. *ACS Nano*. 2018;12(2):1250–1261.
33. Song W, Shen L, Wang Y, et al. Synergistic and low adverse effect cancer immunotherapy by immunogenic chemotherapy and locally expressed PD-L1 trap. *Nat Commun*. 2018;9(1):2237.
34. Amreddy N, Muralidharan R, Babua A, et al. Tumor-targeted and pH-controlled delivery of doxorubicin using gold nanorods for lung cancer therapy. *Int J Nanomed*. 2015;10:6773–6788.
35. Khasraw M, Bell R, Dang C. Epirubicin: is it like doxorubicin in breast cancer? A clinical review. *The Breast*. 2012;21(2):142–149.
36. Suk JS, Xu Q, Kim N, Hanes J, Ensign LM. PEGylation as a strategy for improving nanoparticle-based drug and gene delivery. *Adv Drug Deliv Rev*. 2016;99(Pt A):28–51.
37. Kolate A, Baradia D, Patil S, Vhora I, Kore G, Misra A. PEG – a versatile conjugating ligand for drugs and drug delivery systems. *J Control Release*. 2014;192:67–81.
38. Marrazzo A, Fiorito J, Zappalà L, et al. Antiproliferative activity of phenylbutyrate ester of haloperidol metabolite II [(±)-MRJF4] in prostate cancer cells. *Eur J Med Chem*. 2011;46(1):433–438.
39. Evans JC, Malhotra M, Fitzgerald KA, et al. Formulation and evaluation of Anisamide-Targeted amphiphilic cyclodextrin nanoparticles to promote therapeutic gene silencing in a 3D prostate cancer bone metastases model. *Mol Pharm*. 2017;14(1):42–52.
40. Boyer D, Tamarat P, Maali A, Lounis B, Orrit M. Photothermal imaging of nanometer-sized metal particles among scatterers. *Science*. 2002;297(5584):1160–1163.
41. Guo J, O'Driscoll CM, Holmes JD, Rahme K. Bioconjugated gold nanoparticles enhance cellular uptake: a proof of concept study for siRNA delivery in prostate cancer cells. *Int J Pharm*. 2016;509(1–2):16–27.
42. Ding W, Liu Y, Li Y, et al. Water-soluble gold nanoclusters with pH-dependent fluorescence and high colloidal stability over a wide pH range via co-reduction of glutathione and citrate. *RSC Adv*. 2014;4(43):22651–22659.
43. Freese C, Unger RE, Deller RC, et al. Uptake of poly(2-hydroxypropylmethacrylamide)-coated gold nanoparticles in microvascular endothelial cells and transport across the blood–brain barrier. *Biomacromolecules*. 2013;1(8):824–833.
44. Ju RJ, Zeng F, Liu L, et al. Destruction of vasculogenic mimicry channels by targeting epirubicin plus celecoxib liposomes in treatment of brain glioma. *Int J Nanomedicine*. 2016;11:1131–1146.
45. Lee CM, Tannock IF. Inhibition of endosomal sequestration of basic anticancer drugs: influence on cytotoxicity and tissue penetration. *Br J Cancer*. 2006;94(6):863–869.
46. Hurwitz SJ, Terashima M, Mizunuma N, Slapak CA. Vesicular anthracycline accumulation in doxorubicin-selected U-937 cells: participation of lysosomes. *Blood*. 1997;89(10):3745–3754.
47. Yang X, Fan B, Gao W, et al. Enhanced endosomal escape by photothermal activation for improved small interfering RNA delivery and antitumor effect. *Int J Nanomedicine*. 2018;13:4333–4344.
48. Vermeulen LMP, Fraire JC, Raes L, et al. Photothermally triggered endosomal escape and its influence on transfection efficiency of Gold-Functionalized JetPEI/pDNA nanoparticles. *Int J Mol Sci*. 2018;19(8):pii: E2400.
49. Adams JM, Cory S. The bcl-2 apoptotic switch in cancer development and therapy. *Oncogene*. 2007;26(9):1324–1337.
50. Bredlau AL, McCrackin MA, Motamarry A, et al. Thermal therapy approaches for treatment of brain tumors in animals and humans. *Crit Rev Biomed Eng*. 2016;44(6):443–457.
51. Schaaf L, Schwab M, Ulmer C, et al. Hyperthermia synergizes with chemotherapy by inhibiting PARP1-Dependent DNA replication arrest. *Cancer Res*. 2016;76(10):2868–2875.

Supplementary materials

Synthesis of AuNR-CTAB with longitudinal wavelengths of ~700, 725, and 765 nm

Synthesis of gold nanorods (AuNRs) with longitudinal wavelength (~700 nm): About 75 mL of 0.2 M hexadecyltrimethylammonium bromide (CTAB) solution was added to 0.485 mL of 12.36 mM $AgNO_3$ solution at 25°C, which was followed by the addition of 75 mL of 0.001 M $HAuCl_4$. Afterward, 1.8 mL of 0.0788 M $C_6H_8O_6$ was added, and the solution color changed from dark yellow to colorless. Subsequently, 0.108 mL of the seed solution was added to the growth solution at 27°C–30°C. The solution color changed to dark blue within 5–15 minutes. The growth medium was kept undisturbed at 27°C–30°C for 22 hours. The obtained AuNR-CTAB (~700 nm) complex was washed three times with deionized water by centrifugation (12,500 rpm, 5 minutes) prior to the following experiments.

Synthesis of AuNRs with longitudinal wavelength (~725 nm): About 75 mL of 0.2 M CTAB solution was added to 2.184 mL of 12.36 mM $AgNO_3$ solution at 25°C, which was followed by the addition of 75 mL of 0.001 M $HAuCl_4$. Afterward, 1.8 mL of 0.0788 M $C_6H_8O_6$ was added, and the solution color changed from dark yellow to colorless. Subsequently, 0.108 mL of the seed solution was added to the growth solution at 27°C–30°C. The solution color changed to dark blue within 10–20 minutes. The growth medium was kept undisturbed at 27°C–30°C for 22 hours. The obtained AuNR-CTAB (~725 nm) was washed three times with deionized water by centrifugation (12,500 rpm, 5 minutes) prior to the following experiments.

Synthesis of AuNRs with longitudinal wavelength (~765 nm): About 75 mL of 0.2 M CTAB solution was added to 3 mL of 4 mM $AgNO_3$ solution at 25°C, which was followed by the addition of 75 mL of 0.001 M $HAuCl_4$. Afterward, 1.05 mL of 0.0788 M $C_6H_8O_6$ was added, and the solution color changed from dark yellow to colorless. Subsequently, 0.108 mL of the seed solution was added to the growth solution at 27°C–30°C. The solution color changed to deep red within 15–30 minutes. The growth medium was kept undisturbed at 27°C–30°C for 22 hours. The obtained AuNR-CTAB (~765 nm) was washed three times with deionized water by centrifugation (12,500 rpm, 5 minutes) prior to the following experiments.

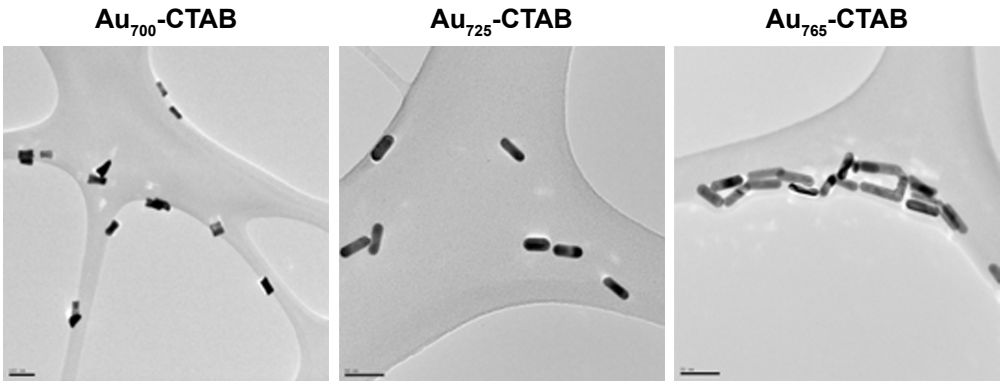

Figure S1 TEM images of Au_{700}-CTAB, Au_{725}-CTAB, and Au_{765}-CTAB (scale bar =50 nm).
Abbreviations: TEM, transmission electron microscopy; Au, gold; CTAB, hexadecyltrimethylammonium bromide.

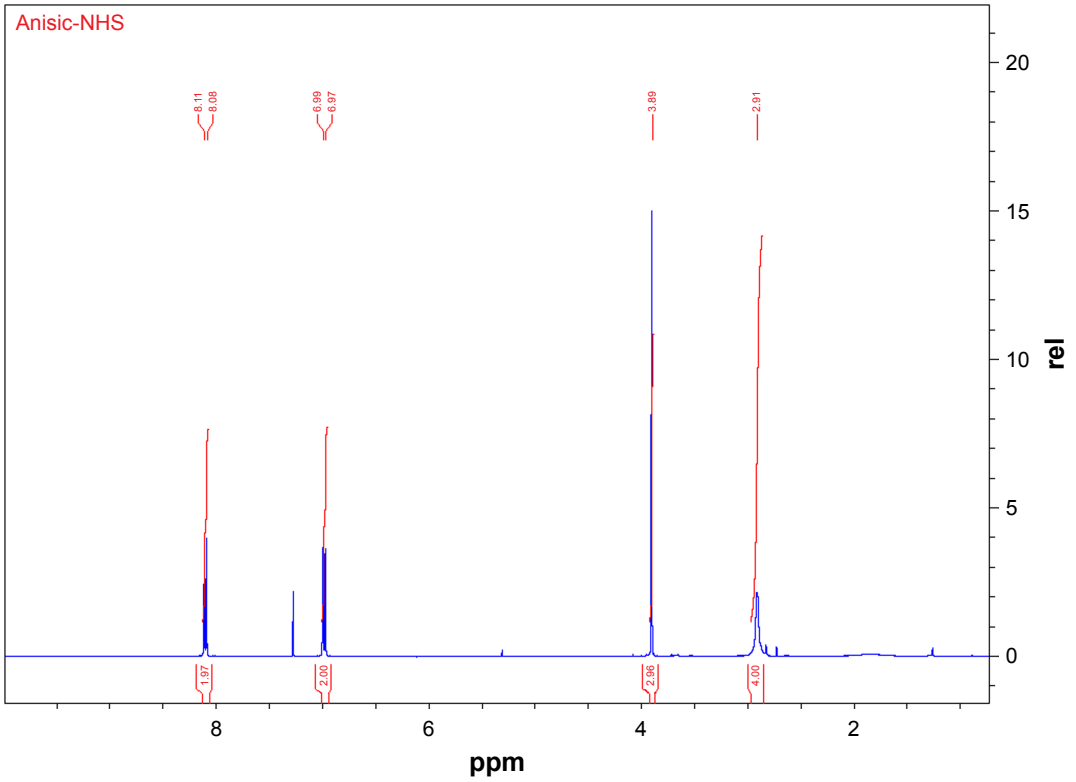

Figure S2 ^{1}H NMR spectrum of anisic-NHS.
Abbreviations: NMR, nuclear magnetic resonance; NHS, N-hydroxysuccinimide.

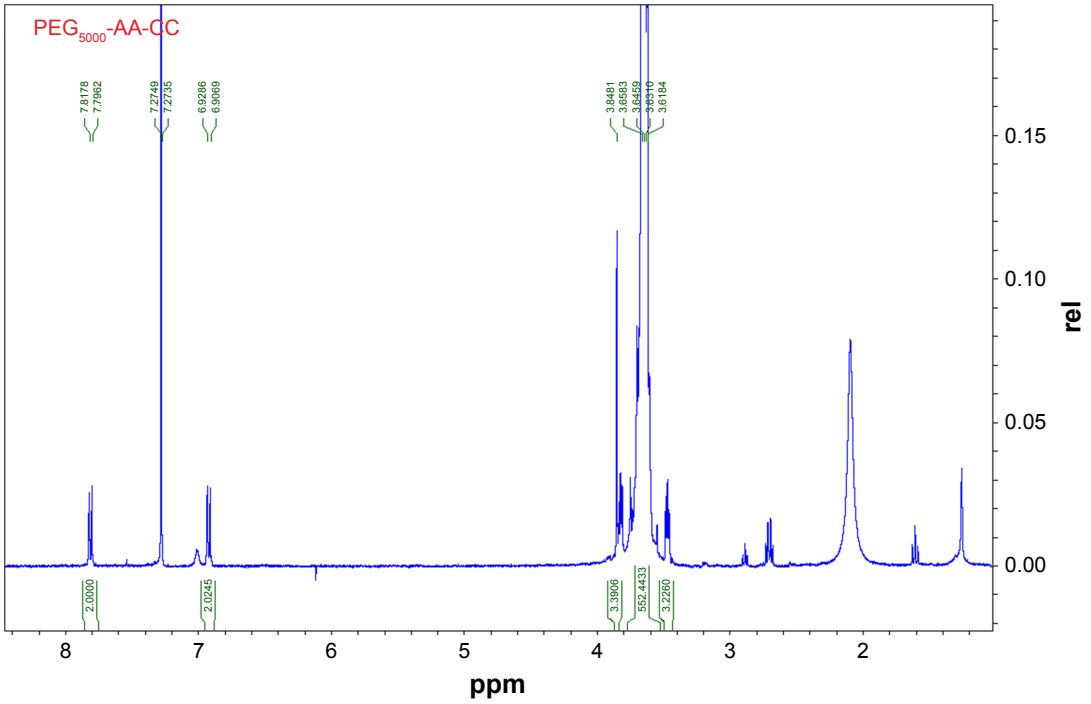

Figure S3 ^{1}H NMR spectrum of SH-PEG$_{5000}$-AA.
Abbreviations: NMR, nuclear magnetic resonance; PEG, polyethylene glycol; AA, anisamide.

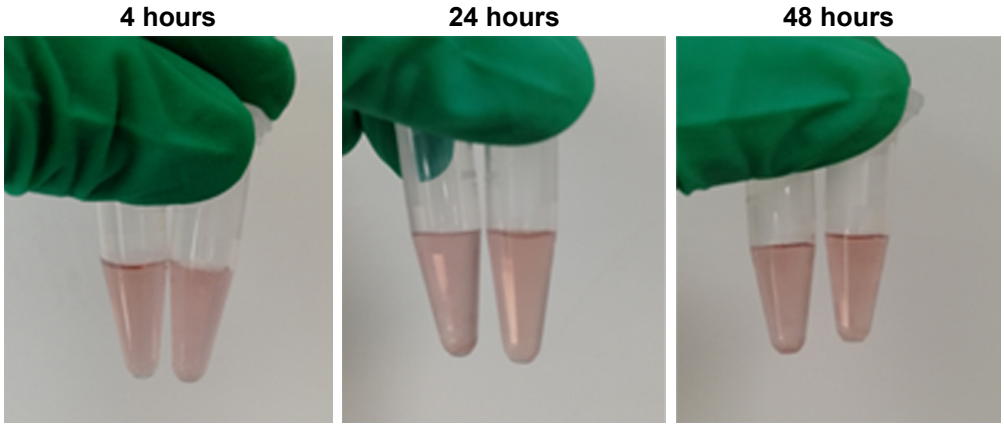

	Time (hours)	Particle size (nm)	Zeta potential (mV)	PDI
37°C	6	88±5	–5±1	0.218
	24	95±7	–5±2	0.221
	48	99±8	–5±2	0.231
4°C	6	90±7	–5±1	0.225
	24	98±5	–7±2	0.235
	48	105±10	–8±2	0.241

Figure S4 Stability of Au_{800}-CTAB-PAA-PEG-AA.EPI complex (MR =5) incubated in the saline at 4°C (left tube in the image) and 37°C (right tube in the image) for 4, 24, and 48 hours. In addition, the size distribution results obtained from dynamic light scattering demonstrated that no aggregation occurred following the incubation.
Abbreviations: Au, gold; CTAB, hexadecyltrimethylammonium bromide; PAA, poly(acrylic acid); AA, anisamide; PEG, polyethylene glycol; EPI, epirubicin; MR, mass ratio; PDI, polydispersity index.

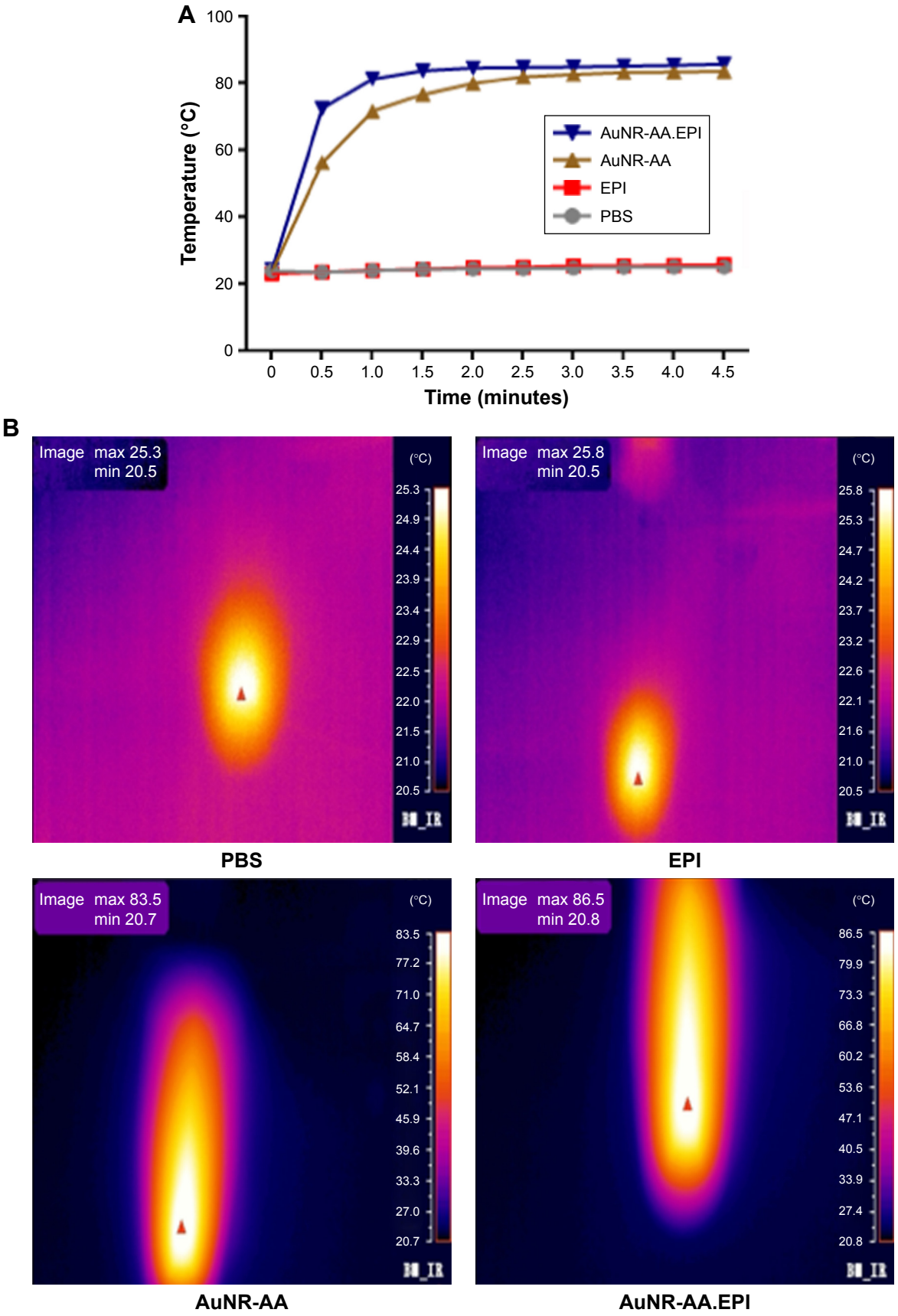

Figure S5 (**A**) Kinetic changes of surface temperature after the laser irradiation (808 nm, 2.5 W/cm^2) of PBS, EPI, Au_{800}-CTAB-PAA-PEG-AA (AuNR-AA), and AuNR-AA.EPI complex for 4.5 minutes. (**B**) Thermographic images of PBS, EPI, AuNR-AA, and AuNR-AA.EPI complex after the laser stimulation (808 nm, 2.5 W/cm^2) for 4.5 minutes.
Abbreviations: Au, gold; CTAB, hexadecyltrimethylammonium bromide; PAA, poly(acrylic acid); AA, anisamide; PEG, polyethylene glycol; EPI, epirubicin.

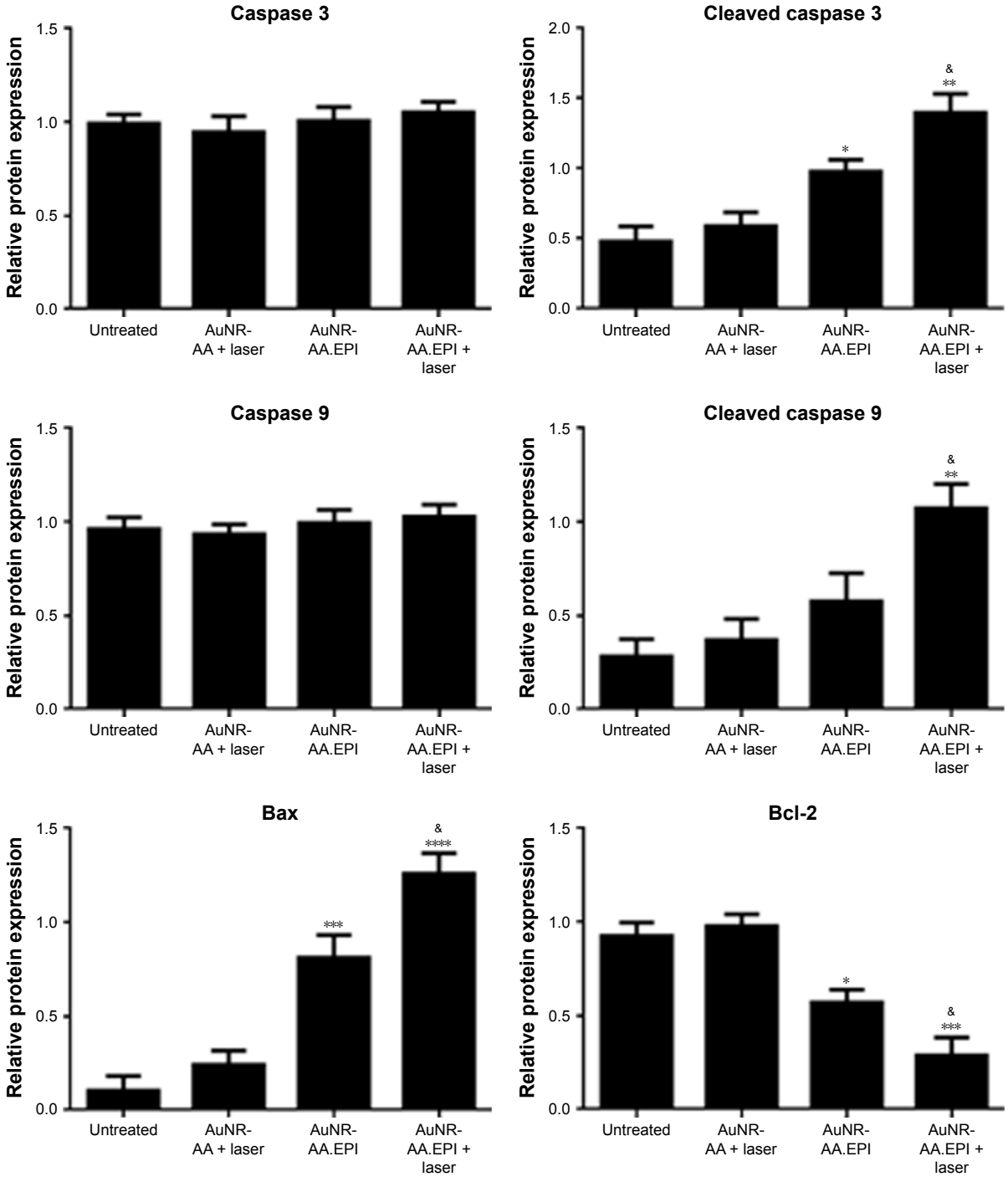

Figure S6 The expression of caspase 3, cleaved caspase 3, caspase 9, cleaved caspase 9, Bax, and Bcl-2 was determined using Western blotting (n=3) relative to β-actin. *P<0.05, **P<0.01, ***P<0.001, ****P<0.0001 relative to the untreated group; &P<0.05 relative to the AuNR-AA.EPI group.

Abbreviations: AuNR, gold nanorod; AA, anisamide; EPI, epirubicin.